Simulation of the Iron Smelting-Reduction Process

K.Sadrnezhaad† *and A.Simchi*
Department of Metallurgical Engineering, Sharif University of Technology, P.O.Box 11365-9466 Tehran, Iran
[Manuscript received July 9, 1998, in revised form October 17, 1998]

A computer program is developed to simulate a two-step smelting-reduction process. Laws of thermodynamics, kinetics, iron-oxide reduction, energy balance, materials balance and transfer of heat and mass between metal, slag and gas are taken into account for development of the model. Local equilibria between metal and slag according to the quadratic formalism of the regular solution model is considered. Dissolution of iron and its oxides in the molten slag and heat transfer from post combustion gases to the molten bath are numerically analyzed. The model is able to evaluate the effect of all important variables on productivity and effectiveness of the process. Special attention is paid to the operational conditions of the reduction furnace while working with the gases coming from a smelter with a high post-combustion ratio and a high reducing-power produced through reforming of the off-gases of the smelter with a natural gas stream in order to minimize the total energy consumption and to maximize the productivity. The application of the model to optimize the behavior of a two stage smelting-reduction system is investigated.

1. Introduction

Designing a continuous reactor for production of liquid metals has several advantages: (1) increasing the ratio of production rate to size, (2) decreasing capital costs, (3) increasing feasibility of construction of small scale melting units, (4) decreasing the costs of transportation, handling and storage of both semi-finished and finished materials, and (5) enabling direct utilization of original raw materials[1].

The process has, however, certain difficulties concerning to (1) low-speed kinetic processes, (2) low-grade refractory materials, (3) unefficient heating facilities and (4) problems associated with dynamic process system design and control[2,3].

A multistage semicontinuous system can, however, be considered as an intermediate solution with lower number of difficulties. Direct smelting of iron is a good example comprising of two consecutive units for pre-reduction and heating and melting processes. Considerable attention has been paid during past 15 years to this method[4,5]. There are, however, a number of shortcomings that must be resolved through further research.

Operational efficiency of the system is influenced by geometry of the vessel, method of charging, rate of feeding, size of particles, use of alternative fuels and their feeding rate, flow rate of gases blown into the vessel and quantities of impurities that come with charge materials into the bath. Effects of these parameters can be determined through evaluation of mass and heat balances, thermodynamics and kinetics of the reactions and fluid flow within and between the phases.

Investigation of these effects is both difficult and expensive if it is aimed to be performed under virtual conditions. Bench scale experimental work is also usually not feasible. Many investigators have therefore simulated the process through application of the physical-mathematical models that may be capable to predict the influence of the important variables[6~8].

There are drastic shortcomings, however, that may inflict these models due to the complexities and lack of thermochemical data. Ideal solution behavior is, for example, a common assumption made by almost all investigators. Practical constraints due to the limited reaction kinetics are generally ignored and constant values are preassigned to the influential variables such as HTC (Heat Transfer Efficiency), PRD (Prereduction Degree) and PCR (Post Combustion Ratio). These are not, however, independent of the rates of consumption of coal, transfer of heat and kinetic processes that occur in the direct smelting reactors.

Regardless of the complexities raised due to the interrelation of the changes and effects, use of computer simulation can facilitate a precise quantitative treatment of the subject. A regular solution model with quadratic formalism can be employed to evaluate balances of materials and energy together with

† To whom correspondence should be addressed

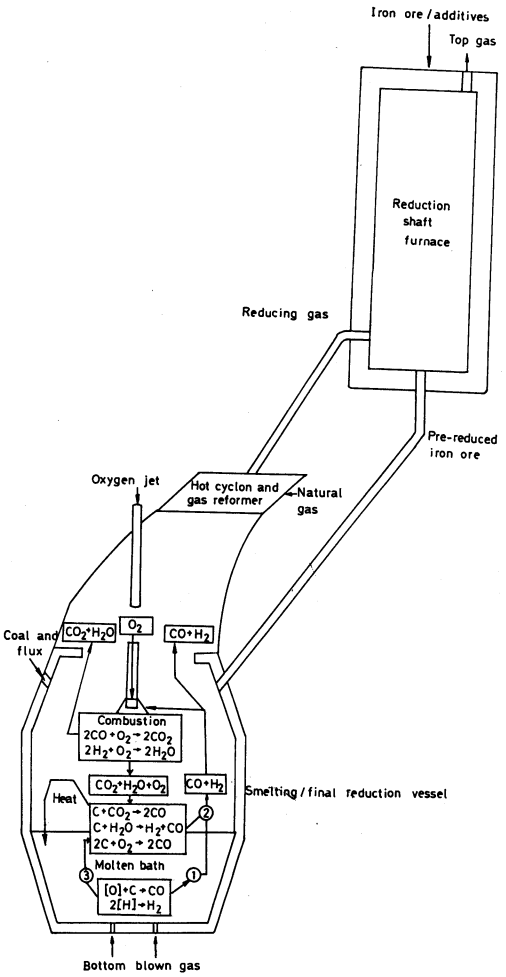

Fig.1 Schematic illustration of double-vessel system used in this research

the thermodynamics and kinetics of the reactions[9]. Efficiency of transfer of heat and mass can be evaluated from reaction kinetics and heat balance calculations[10,11].

In this study, a combined double-vessel process is considered with special attention being paid to geometric design, productivity, effectiveness, energy optimization and economics of the process. Optimum conditions for acquiring the maximum efficiency in heating, reduction, melting and purification of the metal until achieving the desired chemical content can be predicted by application of the model to the special circumstances of interest.

Effective transfer of heat from post combustion reactions, possibility of utilization of both scrap and prereduced ore, additon of alternative fuels, estimation of height of foamy slag, continuous desulfurization and decarburization reactions, evaluation of chemical analyses of the products, presumption of variable geometry and design for prereduction reactor and calculation of productivity of the process all are considered in the model.

2. Modeling

Schematic illustration of the double vessel prereduction/smelting system used in this investigation is shown in Fig.1. The heat that is required for the smelting process is principally provided from oxidation of the coal particles charged into the furnace. The combustion process is performed in the upper part of the smelter. Released enthalpies of the reactions are principally transferred into the molten bath. Reforming of the off-gas can be achieved with employment of a hot cyclon and reformer box that can be installed between the smelter and the prereduction vessel. The prereduction vessel is employed to provide the prereduced materials required to be fed into the smelter.

A stream of natural gas may be injected into the reformer box. Reforming reactions can end-up with an enriched out-flow. Utilization of the out-flow in lower section of the prereduction vessel results in formation of a highly metallized burden. Geometry and design of the prereduction vessel can be changed as a function of the reduction potential and rate of the reformer out-flow.

The first approximation for evaluation of the rates of consumption of materials and energy can be practiced through presumption of unknown system variables such as PRD, HTC, gas temperature (T_g) and coal weight. Partial pressure of the gases are determined from PCR and the equilibrium constant of the reactions occuring in the gaseous phase:

$$\mathrm{PCR} = 100\left(\frac{P_{CO_2} + P_{H_2O}}{P_{CO_2} + P_{H_2O} + P_{CO} + P_{H_2}}\right) \quad (1)$$

$$CO_2 + H_2 \rightarrow CO + H_2O \quad (2)$$

The activities of the components of the slag are determined from quadratic formalism of the regular solution model modified by a "conversion free energy" term ΔG°[9].

$$RT \ln \gamma_i = \Sigma_j \alpha_{ij} X_j^2 + \Sigma_j \Sigma_k (\alpha_{ij} + \alpha_{ik} - \alpha_{jk}) X_j X_k \quad (3)$$

γ_i: activity coefficient of component i of slag
α_{ij}: interaction energy of cations
X_j: mole fraction of component j of slag

$$RT \ln a_i = RT \ln a_{i(\mathrm{R.S})} + \Delta G^{\circ} \quad (4)$$

a_i: activity of component i of slag
$a_{i(\mathrm{R.S})}$: activity of i based on regular solution model

The activities of the components of the metallic phase are determined from first and second interaction parameters[13]. Assuming equilibrium between liquid iron and FeO of the slag, the oxygen content of the molten metal is determined from[14]:

$$\%\underline{O} = 0.6867\Lambda + 0.00296\%\mathrm{FeO} + 0.5106 \quad (5)$$

Table 1 Conversion free energies for important components of steelmaking slags[9]

Reaction	ΔG°/J
$FeO_{(1)}+(1\text{-}t)Fe_{(s\ or\ l)} \rightarrow$"FeO"$_{(R.S)}$	-8 540+7.142 T
$SiO_{2(l)} \rightarrow SiO_{2(R.S)}$	17 450+2.82 T
$MnO_{(l)} \rightarrow MnO_{(R.S)}$	-86 860+51.465 T
$CaO_{(l)} \rightarrow CaO_{(R.S)}$	-40 880−4.703 T
$MgO_{(l)} \rightarrow MgO_{(R.S)}$	-23 300+1.833 T
$P_2O_{5(l)} \rightarrow 2PO_{2.5(R.S)}$	52 720−230.706 T

Table 2 Optical basicity of pure oxides[15]

K_2O	Na_2O	BaO	SrO	Li_2O	CaO	MgO
1.40	1.15	1.15	1.07	1	1	0.78
Al_2O_3	MnO	ZrO_2	TiO_2	Cr_2O_3	V_2O_5	FeO
0.605	0.59	0.59	0.55	0.55	0.53	0.51
Fe_2O_3	SiO_2	B_2O_3	P_2O_5			
0.48	0.48	0.42	0.40			

%O: oxygen content of molten metal

Λ: optical basicity of slag

The quantities of the conversion free energy, the optical basicity of the pure oxides, the free energies associated with the interaction between the cations present in the slag and the first and the second order interaction parameters are listed in Tables 1, 2, 3 and 4, respectively.

The sulfur content of the slag, (%S), is determined based on optical basicity equations[12].

$$\log(\%S) = 0.51\log(\frac{p_{S_2}}{p_{O_2}}) - 13.913 + 42.84\Lambda - 23.82\Lambda^2 \frac{11710}{T} - 0.0222(\%SiO_2) - 0.02275(\%Al_2O_3) \quad (6)$$

$$\Lambda = \Sigma N_i \Lambda_i \quad (7)$$

N_i: equivalent fraction of cation i in slag

Λ_i: optical basicity of pure oxide of cation i

$$N_i = \frac{n_i X_i}{\Sigma n_i X_i} \quad (8)$$

n_i: number of moles of i in compound

For modeling of the post-combustion process, oxidation of CO is considered according to:

$$\overline{m}CO_{(T_M)} + \overline{n}O_{2(298)} \rightarrow \overline{o}CO_{2(T_g)} + (\overline{m} - \overline{o})CO_{(T_g)} + (\overline{n} - 0.5\overline{o})O_{2(T_g)} \quad (9)$$

in which $\overline{m}$ is the flow rate of CO produced at T_M in the reactor and $\overline{n}$ is the rate of blowing of oxygen into the reactor at 298 K and $\overline{o}$ is the rate of production of CO_2 at T_g due to the combustion of CO. These rates are detemined from mass and heat balances in the reactor.

Particle distribution in the gas phase is evaluated from[7]:

$$R_v = 100\ \exp[-(\frac{d}{d'})^n] \quad (10)$$

Table 3 Interaction energies of cations present in steelmaking slags[9]

i \ j	Fe^{2+}	Fe^{3+}	Mn^{2+}	Ca^{2+}	Mg^{2+}	Si^{4+}	P^{5+}	Al^{3+}
Fe^{2+}	-	-18660	7110	-31380	33470	-41840	-31380	-41000
Fe^{3+}	-18660	-	-56480	-95810	-2930	32640	14640	-161080
Mn^{2+}	7110	-56480	-	-92050	61920	-75310	-84940	-83680
Ca^{2+}	-31380	-95810	-92050	-	-100420	-133890	-251040	-154810
Mg^{2+}	33470	-2930	-61920	-100420	-	-66940	-37660	-71130
Si^{4+}	-41840	-32640	-75310	-133890	-66940	-	83680	-127610
P^{5+}	-31380	14640	-84940	-251040	-37660	83680	-	-261500
Al^{3+}	-41000	-161080	-83680	-154810	-71130	-127610	-261500	-

Table 4 First and eliminate second order interaction parameters of elements dissolved in molten iron[16]

e_i^j \ i	j \ r_i^j	C	O	P	S	Si
C		0.14	-0.097	0.051	0.046	0.08
		0.0074	-	0.0041	-	0.0007
O		-0.13	-0.2	0.07	-0.133	-0.131
		0	0	0	0	0
P		0.13	0.13	0.062	0.028	0.12
		-	-	-0.001	-	-0.001
S		0.11	-0.27	0.29	-0.028	0.063
		0.0058	-	0.0006	-0.0009	0.0017
Si		0.18	-0.23	0.11	0.056	0.11
		-	-	-	-	0.0021

in which R_v is mass fraction of droplets with diameters larger than d, and d' is the minimum diameter of the suspended drops. The heat transferred from the gas into the desending droplets can be evaluated from the dynamic behavior of the system. The suspension time of the droplets ($2t_r$) and their decending speed (u) are determined from numerical solution of the following equations:

$$-\frac{1}{6}\pi {d_D}^3 \rho_D \frac{du}{dt} = 3\pi d_D \mu_G (u_G - u) + g\rho_D' \frac{1}{6}\pi {d_D}^3 \qquad \mathrm{Re} \le 1 \tag{11}$$

$$-\frac{1}{6}\pi {d_D}^3 \rho_D \frac{du}{dt} = -\frac{3}{2}\pi {\mu_G}^{1/2} {\rho_G}^{1/2} {d_D}^{3/2} (u_G - u)^{3/2} + g\rho_D \frac{1}{6}\pi {d_D}^3 \qquad \mathrm{Re} > 1 \tag{12}$$

The coefficient of transfer of heat is determined from the correlations between the dimensionless quantities Nu, Pr and Re. The total quantity of heat that transfers into the drops ($\overline{Q}_t$) is evaluated from microkinetics of the heating process:

$$\overline{Q}_t = \Sigma_i \frac{6\overline{M}_D^* v_i}{\rho_D d_{D,i}} \int_0^{t_{r,i}} (h_{r,i} - h_{c,i})(T_G - T_{D,i})dt \tag{13}$$

This heat comes from combustion of the gases (reaction number 9) and is dependent upon macro-kinetics and thermodynamics of the reactions occurring between solid, liquid and the gas phase. Efficiency of transfer of heat from gas into the molten bath is evaluated from:

$$\mathrm{HTC} = \frac{\overline{Q}_t}{\overline{Q}_{t,I}} \tag{14}$$

in which $\overline{Q}_{t,I}$ is the total heat that is generated by the combustion reaction.

The degree of prereduction of the burden can be evaluated from the thermochemistry of the gas-solid reactions. Differential equations describing multistage counter-current plug-flow inside the prereduction vessel are numerically solved to evaluate temperature and composition of gas and solid materials both locally and globally.

Evolution of the gases emanating from the liquid phase results in production of a foamy slag. The height of the slag is related to both the physical properties of the slag and velocity of the gas[17,18].

$$H \propto \frac{\mu_s}{(\rho\sigma)^{1/2}} \cdot \frac{Q}{A} \tag{15}$$

H: height of foamy slag
μ_s: viscosity of slag
ρ: density of slag
σ: surface tension of slag
Q: flow rate of slag
A: surface area of molten metal pool

Detailed descriptions of the properties and their evaluation methods are given in literature [19~21].

The overall process undergoes a number of constraints. Large volumes of gas, for example, cause the formation of an extra ordinary foamy slag that can raise the height of the bath and cause a lower smelter productivity. Excessively high degree of metallization, on the other hand, causes lowering of the height of the bath and decreasing the energy efficiency of the system.

The productivity can also be influenced by extent and mechanisms of the reduction reactions, transport of mass and momentum within and between the phases, dissolution and final reduction of the oxides and removal of the impurity elements from the metallic phase[22]. An example is the rate of reduction of liquid FeO which depends on the iron content of the slag phase[23].

$$\overline{R} = k \cdot \%\mathrm{Fe} \tag{16}$$

$\overline{R}$: semisteel production rate

The rate constant k depends on the amount of agitation in the bath, temperature and volume of the slag and weight of carbon particles suspended in the liquid phase:

$$k = k_1 + (\frac{W_s}{A}) \cdot (k_2 + \frac{W_c}{W_s} k_3)/1000 \tag{17}$$

in which W_s is weight of the slag, W_c is weight of carbon particles suspended in the slag and k_1[= 0.032 kmol $-$ O_2/(min.(%T.Fe).m_2], k_2[= 14 kmol $-$ O_2/(min.(%T.Fe).t $-$ slag] and k_3[= 40 kmol $-$ O_2/(min.(%T.Fe).t $-$ coke] and apparent rate constants at slag/metal, slag/droplets and slag/carbonaceous materials interface, respectively[24].

The thermodynamic data required for calculations are obtained from literature [16, 25 and 26]. The transport properties are given in literature [7,15 and 27]. The flow chart of the simulation model produced in this research is illustrated in Fig.2.

3. Results and Discussion

Model calculations show that the most effective parameters influencing the consumption of materials and energy are PCR and PRD. While these quantities are strongly interrelated, PCR and the rate of injection of oxygen are nearly in proportion. PRD depends both on O_2/CO ratio and reforming of the combusted gas. In order to determine the interrelated effects of these parameter, an 100-ton reactor with specifications summarized in Table 5 is employed.

Figure 3 demonstrates the effect of PCR on PRD and the weight of coal that must be charged into the furnace. Small increases of up to 8% in PCR do not considerably influence the prereduction degree but

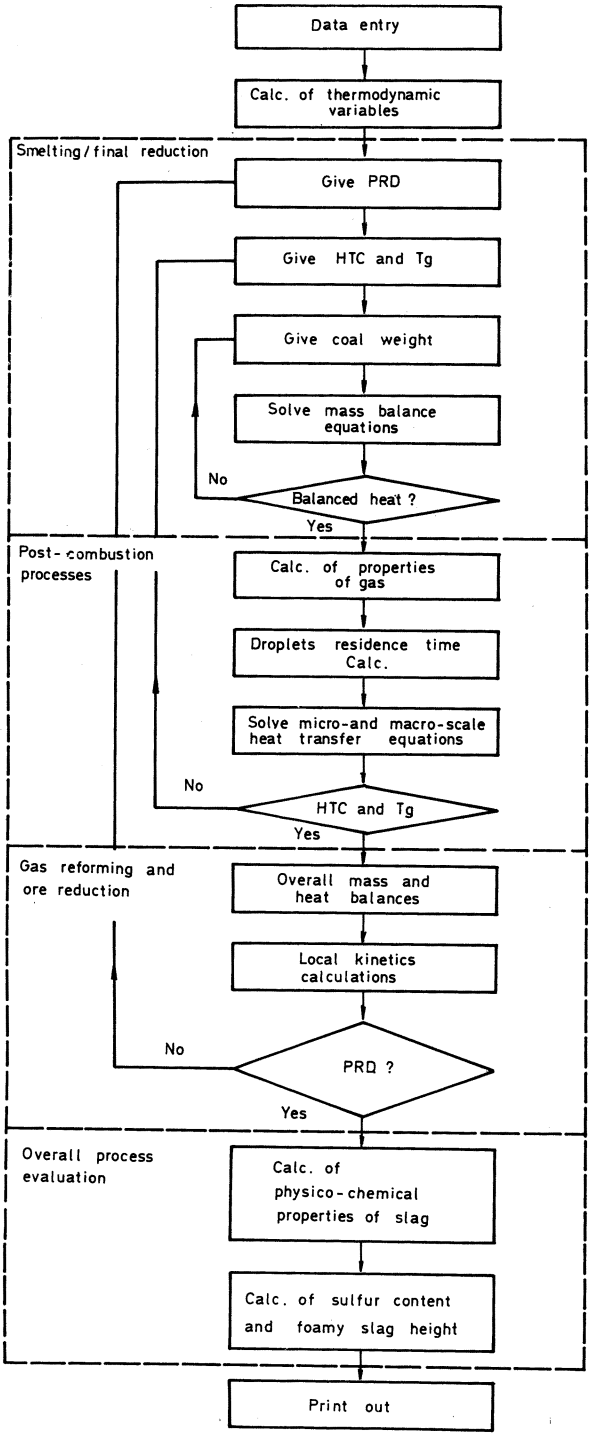

Fig.2 Flow chart of the computer program for simulation of the smelting-reduction process

Table 5 Specifications of a sample of double-vessel smelting-reduction process used for calculations

Parameter	Value
Area of molten metal pool	30 m^2
Temperature of molten metal	1723°C
Carbon content of metallic melt	3.5 wt. pct
Density of molten metal	7000 kg/m^3
Heat capacity of metallic melt	500 J/kg K
Density of gas	0.5 kg/m^3
Minimum diameter of droplets	0.00005 m
Initial speed of droplets	2 m/s
Rate of formation of droplets	550 kg/s
FeO content of slag	5%
Productivity of the process	40 t/h
Prereduction temperature	1123 K
Diameter of prereduction vessel	6 m

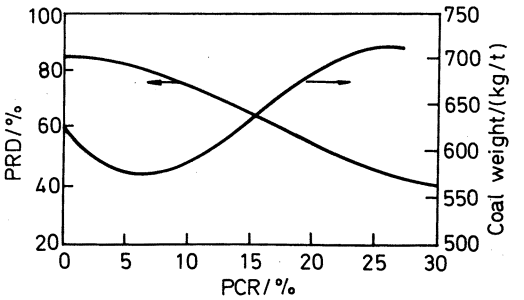

Fig.3 Effect of PCR on PRD and coal consumption in a double-vessel reactor without gas reformer

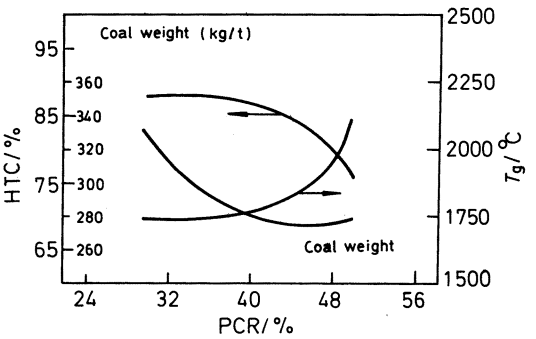

Fig.4 Effect of PCR on HTC, coal consumption and gas temperature in a double-vessel smelting-reduction system with gas reformer

substantially reduces the consumption of coal. Relative insensitivity of PRD may be due to the chemical reserve zones existing in the lower part of the prereduction shaft. The reduction in coal consumption is due to the large release of the combustional heat.

A further increase in PCR results in a sharper decrease in obtainable PRD and a considerable reduction in efficiency of transfer of heat into the molten pool of liquid metal which causes a substantial increase in the rate of consumption of coal. The minimum consumption of coal and the corresponding PCR both represent interesting base lines for designing an optimum combined smelting-reduction unit when reforming of the combusted gas is not to be practiced.

Effect of PCR on HTC, T_g and coal weight in a combined smelting-reduction unit comprizing of the maximum accessible natural-gas-reforming is represented in Fig.4. As is shown in the figure, the consumption of coal can be reduced to about 50% of the

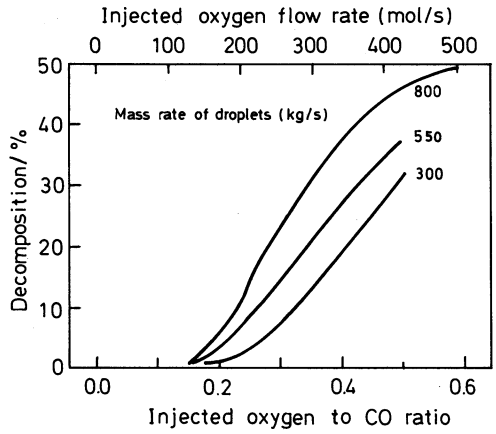

Fig.5 Effect of injection of O_2 and formation of liquid droplets on thermal decomposition of CO_2

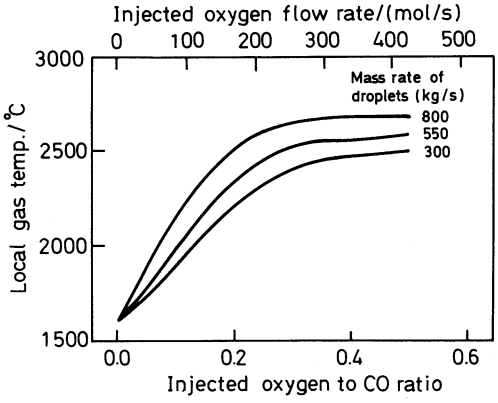

Fig.6 Effect of injection of O_2 and formation of liquid droplets on local gas temperature

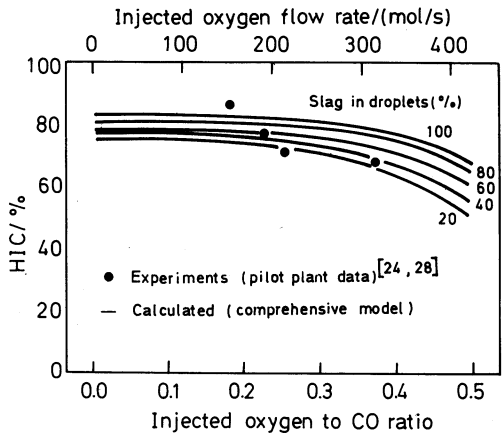

Fig.7 Effect of injection of O_2 and composition of droplets on efficiency of transfer of heat from gas to the melt

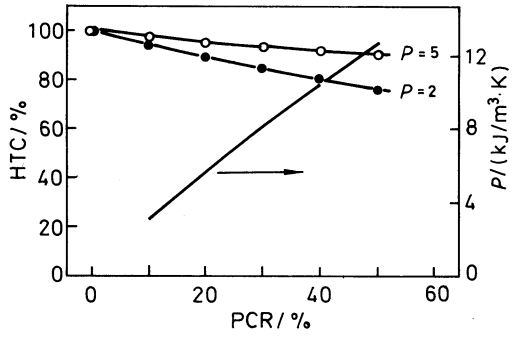

Fig.8 Effect of post combustion ratio and injection surface area on heating efficiency of the system

previous case by the greatest utilization of the thermal energies and subsequent enhancements of PRD through reforming of the off-gas. This can lead the way to a suitable alternative for optimization of material and energy consumptions.

Model calculations show, however, a seizure in reduction of coal weight when PCR exceeds 40%. This is an unfavourable condition which lowers the efficiency of transfer of heat and increases the temperature of the exhausting gas (Fig.4). Under these conditions the destruction of refractory materials by melting and dissociation of CO_2 because of excessive heating can occur in the system(Fig.5).

Simulation results on the effect of PCR on the gas temperature is illustrated in Fig.6. As is shown in the figure, the gas temperature increases with the rate of injection of O_2. Rate of formation of liquid droplets should also increase with the local gas temperature. The liquid droplets play an important role in the formation of a thick layer of slag above the pool of liquid melt. This layer acts as an intermediate phase for transfer of heat from the hot gas to the liquid melt. It should be noted that efficiency of transfer of heat and temperature of gas both depend on production rate and the composition of the droplets(Fig.6 and 7).

A comparison is made in Fig.7 of the computed data with the experimental pilot results obtained by other investigators[24,28]. Based on these data, a deep pool of slag collected on the top of the metallic bath can result in a higher droplet production rate, a lower slag FeO content and a better protection of the metallic melt from reoxidation. This can help a lower S content, a more efficient energy consumption and a greater semi-steel production rate.

Increasing the surface area and the number of oxygen blowing sites improves the heating efficiency of the system (Fig.8) without excessive addition of gas temperature. This is achieved through enhancement of the number of liquid droplets that absorb heat from the gas. The extent and the number of blowing sites are represented by an empirical parameter P that affects on the heating efficiency by :

$$\eta = 100 - 90\left(\frac{\mathrm{PCR}}{100}\right)^{0.9}\frac{1}{P} \qquad (18)$$

This equation clearly indicates that in order to achieve a required combustion ratio, the quantities of P and PCR can be appropriately controlled so that the heating efficiency would not be reduced.

4. Conclusions

A comprehensive computer model is developed for prediction of behavior of a combined bath-smelting prereduction units. Simultaneous transfer of heat from a post-combusted gas to iron or slag droplets suspended in the gas phase and serving as the medium which finally transfers heat to the melt is considered. The variation of temperature and composition of the CO_2 containing gas when mixed and reformed with alternative fuels and its effects on prereduction of the solid burden and the coal consumption rate are taken into account.

The program is capable to evaluate the degree of prereduction, weights of coal, flux, ore, oxygen, natural gas, metallic product and slag, chemical composition of the liquid melt (%S, %C, %P, *etc.)*, temperature, composition and volume of the off-gas, efficiency of transfer of heat and overall productivity of the smelting-reduction unit.

Several conclusions are obtained from application of the model to specific cases of general interest:

(1) If reforming of the post-combusted gas is not in order, excessive post combustion is not desirable.

(2) With application of a natural gas reforming box, it is possible to obtain a PRD of 75% coupled with a post combustion ratio of up to 50% and a minimum consumption of coal. The temperature of the exhausting gas would, however, be too high under these conditions.

(3) For a post combustion ratio of up to 40% without reforming, the efficiency of transfer of heat decreases only slightly.

(4) For post combustion ratios greater than 40%, the efficiency of transfer of heat decreases due to the greater heat loss and the lower proportion of heat that can be absorbed by the liquid phases.

(5) A highly increasing gas temperature is not desirable because it can cause (a) melting of refractory walls, (b) decomposition of CO_2 and (c) diminution of the heat transfer efficiency.

(6) Reforming of the combusted off-gas together with increasing of the extent of blowing sites can improve the utilization of both thermal and chemical gas potentials and achievement of optimum operational conditions.

REFERENCES

[1] K.Sadrnezhaad: *Journal of Engineering, I. R. Iran,* 1990, **3**(1&2), 37.

[2] S.M.Nutter and K.Li: *I&SM,* 1990, **17**(4), 65.

[3] K.Sadrnezhaad and J.F.Elliott: *Iron and Steel International,* 1980, 327.

[4] R.B.Smith: *Met. Mater.,* 1992(9), 491.

[5] J.C.Agarwal: *I&SM,* 1991, **18**(3), 69.

[6] R.J.Fruehan, K.Ito and B.Ozturk: *I&SM,* 1988(11), 83.

[7] L.Zhang and F.Oeters: *Steel Research,* 1991, **62**(3), 95.

[8] K.Sadrnezhaad and A.Simchi: *Memoirs of Faculty of Engineering, Tehran University,* 1995, **56,** 45. (in Persian)

[9] S.Ban-Ya: *ISIJ Int.,* 1993, **33,** 102.

[10] A.Simchi and K.Sadrnezhaad: *"Simulation of Direct Steelmaking Processes", Steel' 75 Symp., Isfahan University of Technology,* Isfahan, Iran, 1996, 146. (in Persian)

[11] A.Simchi, M.A.Ma'sum and A.M.Farmand: "Optimization of Secondary Combustion Processes in Steel Smelting Reactors through Heat and Mass Transfer Models", *First Iranian Metallurgical Engineers Congress,* Science and Tech. Univ. of Iran, 1997, 303. (in Persian)

[12] B.Ozturk, R.Roth and R.J.Fruehan: *ISIJ Int.,* 1994, **34,** 663.

[13] M.Nagamori: *Metall. Trans. B.,* 1989, **20B,** 434.

[14] A.Bergman and A.Gustafsson: *Proc. of 3rd Int. Symp. on Molten Slags and Fluxes,* Glasgow, 1988, 150.

[15] A.Bergman: *Steel Research,* 1990, **61,** 347.

[16] G.K.Sigworth and J.F.Elliott: *Metal Science,* 1974, **8,** 298.

[17] R.Jiang and R.J.Fruehan: *Metall. Trans. B,* 1991, **22B,** 481.

[18] R.E.Roth, R.Jiang and R.J.Fruehan: *I&SM,* 1992(11), 55.

[19] G.Urbain: *Steel Research,* 1987, **58,** 111.

[20] K.Nakashima and K.Mori: *ISIJ Int.,* 1992, **32,** 11.

[21] K.G.Mills: *ISIJ Int.,* 1993, **33,** 148.

[22] K.Sadrnezhaad: *Scientia Iranica,* 1996, **3**(1~3), 113.

[23] T.Ibaraki, M.Kanemote, S.Ogata, H.Katayama and H.Ishikawa: *I&SM,* 1990, (9), 30.

[24] H.Katayama, T.Ohno, M.Yamauchi, M.Matsuo, T.Kawamura and T.Ibaraki: *ISIJ Int.,* 1992, **32,** 95.

[25] I.Brain, O.Knacke and O.Kubaschewski: *Thermochemical Properties of Inorganic Substances,* Spring & Stahleisen, Berlin, 1977.

[26] O.Kubaschewski, E.L.Evans and C.B.Alcock: *Metallurgical Thermochem.,* 5th ed., Pergamon Press, London, 1967.

[27] R.B.Bird, W.E.Stewart and E.N.Lightfood: *Transport Phenomena,* Wiley, NY, 1960.

[28] T.Hirata, M.Ishikawa and S.Anezaki: *ISIJ International,* 1992, **32**(2), 182.